

Position-aided Large-scale MIMO Channel Estimation for High-Speed Railway Communication Systems

Tao Li, Xiaodong Wang, *Fellow, IEEE*, Pingyi Fan, *Senior Member, IEEE*, and Taneli Riihonen, *Member, IEEE*

Abstract

We consider channel estimation for high-speed railway communication systems, where both the transmitter and the receiver are equipped with large-scale antenna arrays. It is known that the throughput of conventional training schemes monotonically decreases with the mobility. Assuming that the moving terminal employs a large linear antenna array, this paper proposes a position-aided channel estimation scheme whereby only a portion of the transmit antennas send pilot symbols and the full channel matrix can be well estimated by using these pilots together with the antenna position information based on the joint spatial-temporal correlation. The relationship between mobility and throughput/DoF is established. Furthermore, the optimal selections of transmit power and time interval partition between the training and data phases as well as the antenna size are presented accordingly. Both analytical and simulation results show that the system throughput with the position-aided channel estimator does not deteriorate appreciably as the mobility increases, which is sharply in contrast with the conventional one.

Index Terms

Large-scale MIMO, high-speed railway communications, linear antenna array, channel estimation, joint spatio-temporal correlation, throughput, degree of freedom (DoF).

T. Li and P. Fan are with Tsinghua National Laboratory for Information Science and Technology (TNList) as well as Department of EE, Tsinghua University, Beijing, P. R. China, 100084 (e-mail: litao12@mails.tsinghua.edu.cn; fpy@tsinghua.edu.cn).

X. Wang is with the Electrical Engineering Department, Columbia University, New York, NY 10027, USA (e-mail: wangx@ee.columbia.edu).

T. Riihonen is with the Department of Signal Processing and Acoustics, Aalto University School of Electrical Engineering, 00076 Aalto, Finland (e-mail: taneli.riihonen@aalto.fi).

I. INTRODUCTION

The large-scale multiple-input multiple-output (MIMO) technology holds the key to significantly improving the throughput of future wireless communication systems [1]. For high-speed railway communication systems, both the base station (BS) and the mobile terminal (i.e., the train) can employ large-scale antenna arrays to provide high-throughput services to users on the train [2–4]. In this paper, we focus on such a high-speed railway MIMO scenario, where both the transmitter and the receiver are equipped with large-scale antenna arrays.

As we know, in MIMO communications, to obtain the instantaneous channel state information (CSI), the training-based channel estimator is widely used. Although the training overhead may be insignificant in single-antenna systems, it becomes the major impediment to high-speed railway MIMO communications, where the speed of the mobile terminal can reach up to hundreds of kilometers per hour [5]. In particular, the throughput of the large-scale MIMO system even can deteriorate to zero if the training phase occupies all the channel uses [6]. It seems very pessimistic to employ large-scale MIMO in highly mobile environments, because the high time-selectivity of the channel removes the benefits brought by multi-antenna wireless links [7, 8].

A rich body of the research in the literature focused on the training-based channel estimation for large-scale MIMO systems under fast fading, see e.g., [9–13]. Specifically, the estimation accuracy in a temporally correlated channel can be improved by employing the Kalman filter [9, 10]. Compressed sensing can be utilized to optimize the delay-Doppler basis of a doubly selective fading channel to improve the estimation accuracy [11]. However, these methods do not aim to reduce the estimation overhead, i.e., the amount of pilots used for channel estimation [9–11]. On the other hand, for a spatially correlated channel, it has been indicated in [12, 13] that the pilot size can be reduced if the number of statistical dominant subspaces is smaller than the number of transmit antennas, at the cost of losing some multiplexing gain. Summarily, it remains a challenging problem to reduce the pilot overhead for large-scale MIMO systems in a high-speed environment.

On the other hand, due to the advances in indoor and outdoor positioning techniques, the

real-time position information of the mobile terminal can be made available. In several prior applications, position information has been already used for routing [14], clustering [15], resource allocation [16, 17], etc. For high-speed railway communications, [18] proposed a position-based channel model and [19] extended the concept to multi-antenna wireless links. Further, position information was utilized to improve the channel estimation accuracy of high-speed railway communications in [20]. An interesting phenomenon caused by the mobility, called the joint spatial-temporal correlation, was discussed in [21–24]. It characterizes the relationship between the channel realizations of distinct antenna pairs at different time due to the mobility of antenna array. In particular, some measurement results between the BS and vehicles with multiple antennas were provided in [21]. [22] discussed the effect of the mutual electromagnetic coupling between different antenna elements. [23] proposed a novel differential modulation for the moving antenna array based on it. [24] discussed the application of spatio-temporal correlation in reducing handover frequency in high-speed railway scenario.

In this paper, we focus on the training-based channel estimation in a large-scale MIMO system under high-speed railway scenarios. It is assumed that the BS is static and the train moves linearly with constant velocity, both employing linear antenna arrays. We mainly consider the uplink channel estimation, while the results can also be used for the downlink due to the channel reciprocity. We find that the joint spatial-temporal correlation can be utilized to significantly reduce the estimation overhead with the help of position information and then propose a position-aided channel estimator. It will be shown that its performance deteriorates a little as the mobility increases. More specifically, during the training phase of each data block, it is better to select a subset of the transmit antennas to send pilot symbols and an initial estimate of the channel submatrix corresponding to this part of transmit antennas can be utilized repeatedly. Later, the estimate of the entire channel matrix could be constructed based on the initial submatrix and the location information of the transmit antenna array, by exploiting the spatial-temporal correlation of the channel. We then analyze its performance in term of the achievable throughput. Finally, we present the optimal selections of system parameters including power allocation, training interval

TABLE I: Some important variables for problem description in this paper.

Variable	Description
M, N	The numbers of transmit antennas and receive antennas
H_k	The channel state matrix during the k -th signal block
$h_{n,m}(k)$	The channel state between m -th transmit antenna and n -th receive antenna
\mathbf{h}_k^m	The channel state vector between m -th transmit antenna and all receive antennas
z_k^m	The position of m -th transmit antenna during the k -th signal block
η	The correlation coefficient between different channel state vector
θ	The moving direction of the terminal with respect to the line-of-sight direction
ψ	The direction of linear antenna array with respect to the line-of-sight direction
$J_0(\cdot)$	The zero-th order Bessel function of the first kind
T_0	The length of each signal block
t_0	The coherence time of the environment

and antenna size, by maximizing the obtained achievable throughput bound in this paper.

It is worth noting that the joint spatial-temporal correlation is significantly different from the conventional spatial correlation or temporal correlation [23]. In this paper, we assume that the antennas are sufficiently separated, so there is no spatial correlation between antenna elements. Besides, under the highly mobile condition, the coherent interval of the channel is so small that the temporal correlation is very weak. The spatial-temporal correlation here refers to the fact that due to the high mobility, the channel responses of different antenna pairs along the moving path at different time are correlated. Hence, the methods and the results based on conventional spatially correlated channel (such as [12]) can not be applied directly here.

The remainder of this paper is organized as follows. The channel model is introduced in Section II, where the joint spatial-temporal correlation is presented. Then, the position-aided channel estimator is developed in Section III. In Section IV, the performance of the system with the new proposed training scheme is analyzed and the optimal system parameter selections are presented. Simulation results are given in Section V. Finally, conclusions are drawn in Section VI.

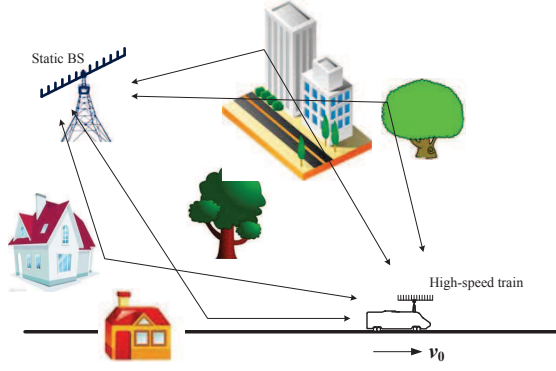


Fig. 1: The large-scale MIMO communication system for high-speed railways.

II. CHANNEL MODEL

As shown in Fig. 1, we consider a point-to-point highly mobile large-scale MIMO system in a high-speed railway, where the BS is static and the terminal is in linear uniform motion with constant velocity v_0 . Suppose that the channel is reciprocal, we concentrate on the uplink channel estimation problem and the results can be directly used in the downlink. According to the training-based system architecture, each signal block is divided into two parts: training phase and data phase. Some known training symbols are sent by the transmitter to estimate the CSI during the training phase and then the estimated channel is used in the following data phase. It is assumed that the channel state keeps constant during the same block, and changes to other values between different blocks. Besides, let the carrier wavelength be λ_0 and symbol rate be B_0 , then the maximum Doppler shift is $f_D = \frac{v_0}{\lambda_0}$, the coherence time of the channel is $\frac{\lambda_0 B_0}{2v_0}$, and the length of each signal block is set as $T_0 = \lfloor \frac{\lambda_0 B_0}{2\xi_0 v_0} \rfloor$ symbols (where the constant ξ_0 should satisfy $\xi_0 \gg 1$).

We assume that a linear antenna array is employed at the mobile terminal (i.e., the train). The number of transmit antennas and receive antennas are denoted as M and N , respectively. We focus on the effects of small-scale fast fading, which is modeled as Rayleigh distribution in this paper. Let $\mathbf{H}_k \in \mathbb{C}^{N \times M}$ be the channel matrix for the k -th signal block with its elements $h_{n,m}(k)$ denoting the channel state between the n -th receive antenna and the m -th transmit

antenna (where $h_{n,m}(k) \sim \mathcal{CN}(0, 1)$). It is assumed that the distance between adjacent antennas is $\frac{\lambda_0}{2}$, so there is no spatial correlation between the antenna elements and the elements in \mathbf{H}_k are i.i.d. Further, let $\mathbf{h}_k^m \in \mathbb{C}^{N \times 1}$ denote the channel vector between the m -th transmit antenna and all N receive antennas in the k -th block, namely $\mathbf{H}_k = [\mathbf{h}_k^1, \mathbf{h}_k^2, \dots, \mathbf{h}_k^M]$. Consequently, these M channel vectors are independent of each other.

Next we introduce the concept of joint spatio-temporal correlation. As shown in Fig. 2, the moving direction of the terminal is θ with respect to the line-of-sight direction, and the direction of the linear antenna array is ψ . Fig. 2 depicts the specific locations of the entire moving antenna array of transmitter at the k_1 -th and k_2 -th signal blocks. It can be seen that the first antenna of the transmitter to the right at the k_1 -th block is located at nearly the same place as the second transmit antenna at the k_2 -th block due to the mobility of terminal. The corresponding channel vectors are $\mathbf{h}_{k_1}^1$ and $\mathbf{h}_{k_2}^2$. Intuitively, there exists some correlation between $\mathbf{h}_{k_1}^1$ and $\mathbf{h}_{k_2}^2$ according to many channel models, such as the Clark's model [27, Sec 2.4]. Such correlation is termed as joint spatio-temporal correlation, which captures the correlation between distinct antenna pairs at different time due to mobility. In general, the specific correlation between $\mathbf{h}_{k_1}^1$ and $\mathbf{h}_{k_2}^2$ can be estimated from measurement. Here, we introduce an analytical model. Specifically, when the moving scattering objects are modeled by poisson point process, the final correlation coefficient between $\mathbf{h}_{k_1}^1$ and $\mathbf{h}_{k_2}^2$ can be expressed as follows (see more details in [23, 25] and the measurements can be found in [21, 22])

$$\eta = \frac{J_0(\sqrt{a^2 + b^2 - \kappa^2 - 2ab \cos(\psi - \theta) + j2\kappa[a \cos(\mu - \theta) + b \cos(\mu - \psi)]})}{J_0(\kappa)}, \quad (1)$$

where $J_0(\cdot)$ is the zero-th order Bessel function of the first kind; κ indicates the width of angle of the arrival (AOA) and μ accounts the mean direction of AOA; $a = 2\pi f_D \tau$ and $b = 2\pi D / \lambda_0$, with τ being the time interval between the k_1 -th and k_2 -th blocks, and D being the antenna spacing.

Assuming that the mobile terminal can adapt the direction of antenna array so that $\psi = \theta$ to achieve the largest correlation. And the scattering is isotropic so we have $\kappa = 0$. Hence, the

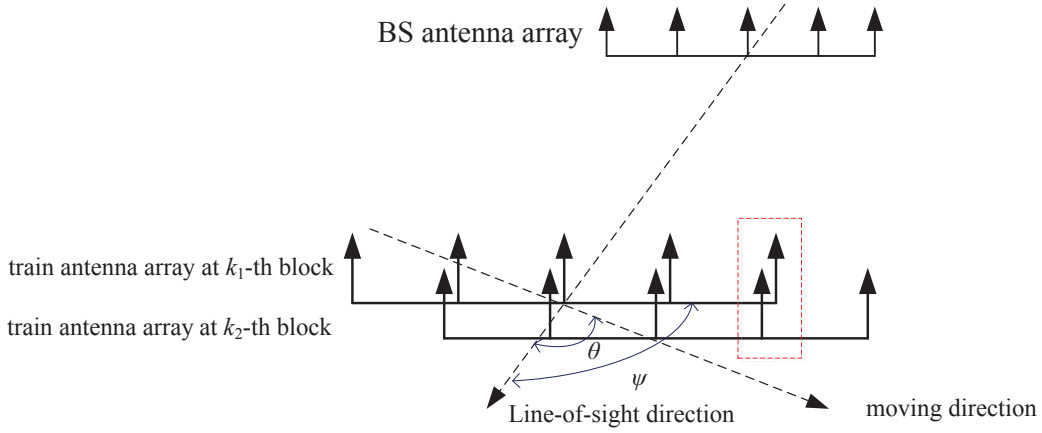


Fig. 2: The joint spatio-temporal correlation of moving antenna array [23].

correlation can be simplified as

$$\eta = J_0(\sqrt{a^2 + b^2 - 2ab \cos(\psi - \theta)}) = J_0\left(\frac{2\pi|v_0\tau - D|}{\lambda_0}\right). \quad (2)$$

Denote the location of the first transmit antenna at the k_1 -th block as $z_{k_1}^1$ and the location of second antenna at the k_2 -th block as $z_{k_2}^2$. Then, we have $|v_0\tau - D| = |z_{k_2}^2 - z_{k_1}^1|$. Consequently, we can extend (2) as the correlation expression between the response of first antenna at the k_1 -th block $\mathbf{h}_{k_1}^1$ and the response of m -th antenna at the k_m -th block $\mathbf{h}_{k_m}^m$ as

$$\eta(z_{k_1}^1, z_{k_m}^m) = J_0\left(\frac{2\pi|z_{k_m}^m - z_{k_1}^1|}{\lambda_0}\right). \quad (3)$$

We assume that the relative position of the transmit antenna array is precisely known at any time, so is the correlation in (3). Besides, we make the following assumption.

Assumption 1: *The channel state at a fixed position within the fading field stays constant during a period t_0 and after that may change to some other value, where t_0 is called the coherence time of the environment and determined by the time variation of the scatterers.*

Remark 1: It is worth noting that the channel coherence time $\frac{\lambda_0}{2v_0}$ and the environment coherence time t_0 are fundamentally different. The former is determined by the moving speed of the transmitter while the latter is by the time variation of the scatterers in the radio propagation paths. In general, $\frac{\lambda_0}{2v_0} \ll t_0$ since the environment can not change much within a short period.

III. POSITION-AIDED CHANNEL ESTIMATION

In the conventional approach, the entire channel matrix is re-estimated in each block, to cope with the channel variation caused by high mobility. Thereby, in order to estimate the channel vectors of M transmit antennas, at least M pilot symbols need to be transmitted during training phase, which leads to huge training overhead in a large-scale MIMO system [6]. To reduce the training overhead, we propose a new channel estimation concept, called position-aided channel estimation, by exploiting the property of joint spatio-temporal correlation. It is assumed that all transmit antennas form a linear array with uniform interval $\frac{\lambda_0}{2}$ and that they move along the same path. Then during the training phase of each block, we have to only estimate the channel vectors of a subset of the transmit antennas by transmitting pilot symbols, while the rest of the channel vectors can be obtained through linear interpolation based on the joint spatial-temporal correlation. As a result, the overhead of the training stage of each block can be significantly reduced, resulting in high data throughput.

A. Initial Estimation of the First Column in Each Group Based on Pilots

Let $\mathbf{h}_k^m \in \mathbb{C}^{N \times 1}$ denote the channel vector between the m -th transmit antenna and all N receive antennas in the k -th block, thus $\mathbf{H}_k = [\mathbf{h}_k^1, \mathbf{h}_k^2, \dots, \mathbf{h}_k^M]$. These M channel vectors are further divided into M_g groups, each containing M_e adjacent columns in \mathbf{H}_k . Thus, $M = M_e \cdot M_g$. Then, the channel sub-matrix for the i -th group can be expressed as

$$\mathbf{Q}_k^i = [\mathbf{q}_{k,i}^1, \mathbf{q}_{k,i}^2, \dots, \mathbf{q}_{k,i}^{M_e}] = [\mathbf{h}_k^{M_e(i-1)+1}, \mathbf{h}_k^{M_e(i-1)+2}, \dots, \mathbf{h}_k^{M_e(i-1)+M_e}], \quad i = 1, 2, \dots, M_g. \quad (4)$$

And the channel matrix \mathbf{H}_k can be rewritten as

$$\mathbf{H}_k = [\mathbf{Q}_k^1, \mathbf{Q}_k^2, \dots, \mathbf{Q}_k^{M_g}]. \quad (5)$$

Under the position-aided channel estimation scheme, only the first transmit antenna in each group sends pilot symbols to estimate the channel state during each block, which corresponds to the following $N \times M_g$ sub-matrix of \mathbf{H}_k :

$$\mathbf{G}_k = [\mathbf{g}_k^1, \mathbf{g}_k^2, \dots, \mathbf{g}_k^{M_g}] = [\mathbf{h}_k^1, \mathbf{h}_k^{M_e+1}, \dots, \mathbf{h}_k^{M_e(M_g-1)+1}]. \quad (6)$$

Denote T_τ as the training duration in terms of the number of pilot symbols, and let $\mathbf{S}_{\tau,k} \in \mathbb{C}^{M_g \times T_\tau}$ and $\mathbf{Y}_{\tau,k} \in \mathbb{C}^{N \times T_\tau}$ be the pilot symbol matrix and the corresponding received signal during the training phase, respectively. Then, the training phase can be modeled as

$$\mathbf{Y}_{\tau,k} = \sqrt{\frac{P_\tau}{M_g}} \mathbf{G}_k \mathbf{S}_{\tau,k} + \mathbf{V}_{\tau,k}, \quad (7)$$

where P_τ is the transmit power during the training phase and $\mathbf{V}_{\tau,k} \in \mathbb{C}^{N \times T_\tau}$ represents additive white Gaussian noise with i.i.d. $\mathcal{CN}(0, 1)$ elements.

The minimum mean-square error (MMSE) estimate of \mathbf{G}_k is given by

$$\hat{\mathbf{G}}_k = \sqrt{\frac{M_g}{P_\tau}} \mathbf{Y}_{\tau,k} \mathbf{S}_{\tau,k}^H \left(\frac{M_g}{P_\tau} \mathbf{I}_{M_g} + \mathbf{S}_{\tau,k} \mathbf{S}_{\tau,k}^H \right)^{-1}. \quad (8)$$

With orthogonal pilot symbol sequences, i.e., $\mathbf{S}_{\tau,k} \mathbf{S}_{\tau,k}^H = \mathbf{I}_{M_g} T_\tau$, substituting (7) into (8), we get

$$\hat{\mathbf{G}}_k = \frac{\frac{P_\tau T_\tau}{M_g}}{1 + \frac{P_\tau T_\tau}{M_g}} \mathbf{G}_k + \frac{\sqrt{\frac{P_\tau T_\tau}{M_g}}}{1 + \frac{P_\tau T_\tau}{M_g}} \mathbf{V}'_{\tau,k}, \quad (9)$$

where $\mathbf{V}'_{\tau,k} = \frac{1}{\sqrt{T_\tau}} \mathbf{V}_{\tau,k} \mathbf{S}_{\tau,k}^H$, the elements of which are still i.i.d. $\mathcal{CN}(0, 1)$.

Let $\hat{\mathbf{G}}_k = [\hat{\mathbf{g}}_k^1, \hat{\mathbf{g}}_k^2, \dots, \hat{\mathbf{g}}_k^{M_g}]$ and $\mathbf{V}'_{\tau,k} = [\mathbf{v}_k^1, \mathbf{v}_k^2, \dots, \mathbf{v}_k^{M_g}]$. Then

$$\hat{\mathbf{g}}_k^i = \frac{\frac{P_\tau T_\tau}{M_g}}{1 + \frac{P_\tau T_\tau}{M_g}} \mathbf{g}_k^i + \frac{\sqrt{\frac{P_\tau T_\tau}{M_g}}}{1 + \frac{P_\tau T_\tau}{M_g}} \mathbf{v}_k^i, \quad i = 1, 2, \dots, M_g. \quad (10)$$

Hence, we have these initial estimates of the first channel column vectors that are independent and identical distributed as

$$\hat{\mathbf{g}}_k^i \sim \mathcal{CN} \left(0, \frac{\frac{P_\tau T_\tau}{M_g}}{1 + \frac{P_\tau T_\tau}{M_g}} \mathbf{I}_N \right), \quad i = 1, 2, \dots, M_g. \quad (11)$$

Let $z_k^{(M_e(i-1)+1)}$ be the position of the first transmit antenna in the i -th group of the k -th signal block over the moving path. Then, $\hat{\mathbf{g}}_k^i$ can be regarded as the CSI sample at the point $z_k^{(M_e(i-1)+1)}$ on the moving path. As shown in Fig. 3, a group of CSI samples along the moving path can be obtained over time k . We then establish the following CSI table Φ_k^i for the i -th group

$$\Phi_k^i = \left\{ (\hat{\mathbf{g}}_l^i, z_l^{(M_e(i-1)+1)}), l = 1, 2, \dots, k \right\}, \quad i = 1, 2, \dots, M_g, \quad (12)$$

which can be used to obtain the estimates of all channel vectors in the i -th group, i.e., $\hat{\mathbf{Q}}_k^i$. The details of this will be given in the sequel.

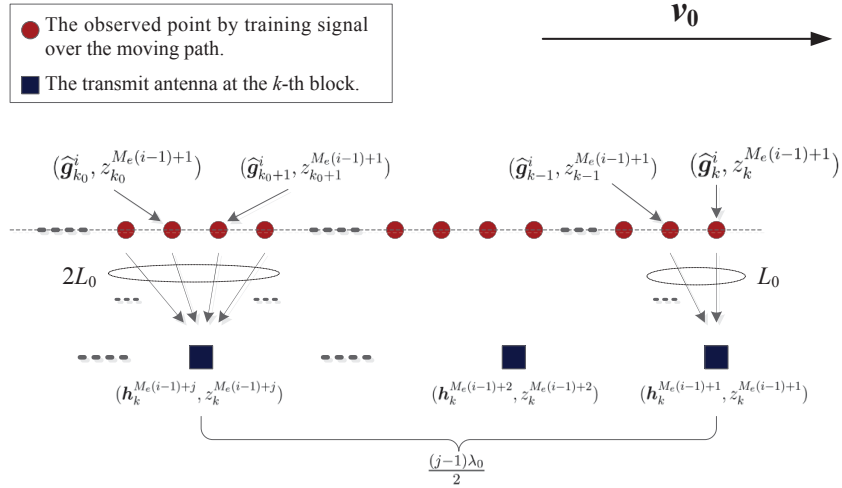


Fig. 3: The diagram of the estimation process for the i -th group under the proposed position-aided channel estimation scheme.

B. Refined Estimation of the First Column in Each Group

As shown in Fig. 3, we will use L_0 samples $\{\widehat{\mathbf{g}}_{k-L_0+1}^i, \dots, \widehat{\mathbf{g}}_{k-1}^i, \widehat{\mathbf{g}}_k^i\}$ over the moving path to refine the estimate of $\mathbf{h}_k^{(M_e(i-1)+1)} = \mathbf{g}_k^i$ with the help of position information (where $L_0 \leq \xi_0$ due to the constraint of channel coherence distance). For notational simplicity, we denote $i_0 = M_e(i-1) + 1$ in this subsection.

As stated in the previous section, $\mathbf{g}_{k-L_0+1}^i, \dots, \mathbf{g}_{k-1}^i$ and \mathbf{g}_k^i are jointly Gaussian distributed with zero mean and the following covariance matrix:

$$\begin{aligned} \mathbf{R}_{\mathbf{g}_k^i, \mathbf{g}_{k-1}^i, \dots, \mathbf{g}_{k-L_0+1}^i} &= \begin{pmatrix} \mathbf{R}_{\mathbf{g}_k^i} & \mathbf{R}_{\mathbf{g}_k^i \mathbf{g}_{k-1}^i} & \cdots & \mathbf{R}_{\mathbf{g}_k^i \mathbf{g}_{k-L_0+1}^i} \\ \mathbf{R}_{\mathbf{g}_{k-1}^i \mathbf{g}_k^i} & \mathbf{R}_{\mathbf{g}_{k-1}^i} & \cdots & \mathbf{R}_{\mathbf{g}_{k-1}^i \mathbf{g}_{k-L_0+1}^i} \\ \vdots & & \ddots & \\ \mathbf{R}_{\mathbf{g}_{k-L_0+1}^i \mathbf{g}_k^i} & \mathbf{R}_{\mathbf{g}_{k-L_0+1}^i \mathbf{g}_{k-1}^i} & \cdots & \mathbf{R}_{\mathbf{g}_{k-L_0+1}^i} \end{pmatrix} \\ &= \begin{pmatrix} \eta_{1,1} & \eta_{1,2} & \cdots & \eta_{1,L_0} \\ \eta_{2,1} & \eta_{2,2} & \cdots & \eta_{2,L_0} \\ \vdots & & \ddots & \\ \eta_{L_0,1} & \eta_{L_0,2} & \cdots & \eta_{L_0,L_0} \end{pmatrix} \otimes \mathbf{I}_N, \end{aligned} \quad (13)$$

where \otimes denotes the Kronecker product and $\mathbf{R}_{\mathbf{x}\mathbf{y}} = \mathbb{E}\{(\mathbf{x} - \mathbb{E}[\mathbf{x}])(\mathbf{y} - \mathbb{E}[\mathbf{y}])^H\}$. By plugging

the location expressions into (3), we have

$$\eta_{m,n} = J_0 \left(2\pi |m - n| \frac{v_0 T_0}{\lambda_0 B_0} \right). \quad (14)$$

However, the receiver does not know the exact values of $\{\mathbf{g}_{k-L_0+1}^i, \dots, \mathbf{g}_{k-1}^i, \mathbf{g}_k^i\}$, but only has their initial estimates based on pilot symbols, namely $\{\widehat{\mathbf{g}}_{k-L_0+1}^i, \dots, \widehat{\mathbf{g}}_{k-1}^i, \widehat{\mathbf{g}}_k^i\}$. Based on (10), $\{\widehat{\mathbf{g}}_{k-L_0+1}^i, \widehat{\mathbf{g}}_{k-L_0+2}^i, \dots, \widehat{\mathbf{g}}_k^i, \mathbf{g}_k^i\}$ are also jointly Gaussian distributed with covariance matrix (recall that $\mathbf{h}_k^{i_0} = \mathbf{g}_k^i$)

$$\begin{aligned} \mathbf{R}_{\mathbf{h}_k^{i_0}, \widehat{\mathbf{g}}_k^i, \dots, \widehat{\mathbf{g}}_{k-L_0+1}^i} &= \begin{pmatrix} \mathbf{R}_{\mathbf{g}_k^i} & \mathbf{R}_{\mathbf{g}_k^i \widehat{\mathbf{g}}_k^i} & \mathbf{R}_{\mathbf{g}_k^i \widehat{\mathbf{g}}_{k-1}^i} & \cdots & \mathbf{R}_{\mathbf{g}_k^i \widehat{\mathbf{g}}_{k-L_0+1}^i} \\ \mathbf{R}_{\widehat{\mathbf{g}}_k^i \mathbf{g}_k^i} & \mathbf{R}_{\widehat{\mathbf{g}}_k^i} & \mathbf{R}_{\widehat{\mathbf{g}}_k^i \widehat{\mathbf{g}}_{k-1}^i} & \cdots & \mathbf{R}_{\widehat{\mathbf{g}}_k^i \widehat{\mathbf{g}}_{k-L_0+1}^i} \\ \mathbf{R}_{\widehat{\mathbf{g}}_{k-1}^i \mathbf{g}_k^i} & \mathbf{R}_{\widehat{\mathbf{g}}_{k-1}^i \widehat{\mathbf{g}}_k^i} & \mathbf{R}_{\widehat{\mathbf{g}}_{k-1}^i} & \cdots & \mathbf{R}_{\widehat{\mathbf{g}}_{k-1}^i \widehat{\mathbf{g}}_{k-L_0+1}^i} \\ \vdots & & & \ddots & \\ \mathbf{R}_{\widehat{\mathbf{g}}_{k-L_0+1}^i \mathbf{g}_k^i} & \mathbf{R}_{\widehat{\mathbf{g}}_{k-L_0+1}^i \widehat{\mathbf{g}}_k^i} & \mathbf{R}_{\widehat{\mathbf{g}}_{k-L_0+1}^i \widehat{\mathbf{g}}_{k-1}^i} & \cdots & \mathbf{R}_{\widehat{\mathbf{g}}_{k-L_0+1}^i} \end{pmatrix} \\ &= \begin{pmatrix} 1 & \eta_{1,1}\sigma_0^2 & \eta_{1,2}\sigma_0^2 & \cdots & \eta_{1,L_0}\sigma_0^2 \\ \eta_{1,1}\sigma_0^2 & \eta_{1,1}\sigma_0^2 & \eta_{1,2}\sigma_0^4 & \cdots & \eta_{1,L_0}\sigma_0^4 \\ \eta_{2,1}\sigma_0^2 & \eta_{2,1}\sigma_0^4 & \eta_{2,2}\sigma_0^2 & \cdots & \eta_{2,L_0}\sigma_0^4 \\ \vdots & & & \ddots & \\ \eta_{L_0,1}\sigma_0^2 & \eta_{L_0,1}\sigma_0^4 & \eta_{L_0,2}\sigma_0^4 & \cdots & \eta_{L_0,L_0}\sigma_0^2 \end{pmatrix} \otimes \mathbf{I}_N, \end{aligned} \quad (15)$$

where

$$\sigma_0^2 = \frac{\frac{P_\tau T_\tau}{M_g}}{1 + \frac{P_\tau T_\tau}{M_g}}. \quad (16)$$

Given the initial estimates in the CSI table Φ_k^i , the MMSE estimate of $\mathbf{h}_k^{i_0}$ is [30]

$$\begin{aligned} \widehat{\mathbf{h}}_k^{i_0} &= \mathbb{E} \left\{ \mathbf{h}_k^{i_0} \middle| \widehat{\mathbf{g}}_{k-L_0+1}^i, \widehat{\mathbf{g}}_{k-L_0+2}^i, \dots, \widehat{\mathbf{g}}_k^i \right\} \\ &= \begin{pmatrix} \eta_{1,1}\sigma_0^2 \\ \eta_{1,2}\sigma_0^2 \\ \vdots \\ \eta_{1,L_0}\sigma_0^2 \end{pmatrix}^T \begin{pmatrix} \eta_{1,1}\sigma_0^2 & \eta_{1,2}\sigma_0^4 & \cdots & \eta_{1,L_0}\sigma_0^4 \\ \eta_{2,1}\sigma_0^4 & \eta_{2,2}\sigma_0^2 & \cdots & \eta_{2,L_0}\sigma_0^4 \\ \vdots & & \ddots & \\ \eta_{L_0,1}\sigma_0^4 & \eta_{L_0,2}\sigma_0^4 & \cdots & \eta_{L_0,L_0}\sigma_0^2 \end{pmatrix}^{-1} \otimes \mathbf{I}_N \begin{pmatrix} \widehat{\mathbf{g}}_k^i \\ \widehat{\mathbf{g}}_{k-1}^i \\ \vdots \\ \widehat{\mathbf{g}}_{k-L_0+1}^i \end{pmatrix}. \end{aligned} \quad (17)$$

And the corresponding MMSE matrix is [30]

$$\begin{aligned} & \mathbb{E} \left\{ \left(\mathbf{h}_k^{i_0} - \widehat{\mathbf{h}}_k^{i_0} \right) \left(\mathbf{h}_k^{i_0} - \widehat{\mathbf{h}}_k^{i_0} \right)^H \right\} \\ &= \mathbf{I}_N - \begin{pmatrix} \eta_{1,1}\sigma_0^2 \\ \eta_{1,2}\sigma_0^2 \\ \vdots \\ \eta_{1,L_0}\sigma_0^2 \end{pmatrix}^T \begin{pmatrix} \eta_{1,1}\sigma_0^2 & \eta_{1,2}\sigma_0^4 & \cdots & \eta_{1,L_0}\sigma_0^4 \\ \eta_{2,1}\sigma_0^4 & \eta_{2,2}\sigma_0^2 & \cdots & \eta_{2,L_0}\sigma_0^4 \\ \vdots & \vdots & \ddots & \vdots \\ \eta_{L_0,1}\sigma_0^4 & \eta_{L_0,2}\sigma_0^4 & \cdots & \eta_{L_0,L_0}\sigma_0^2 \end{pmatrix}^{-1} \begin{pmatrix} \eta_{1,1}\sigma_0^2 \\ \eta_{2,1}\sigma_0^2 \\ \vdots \\ \eta_{L_0,1}\sigma_0^2 \end{pmatrix} \otimes \mathbf{I}_N. \end{aligned} \quad (18)$$

Specifically, when $L_0 = 1$, the MMSE estimate in (17) can be simplified to

$$\widehat{\mathbf{h}}_k^{i_0} = \widehat{\mathbf{g}}_k^i, \quad i = 1, 2, \dots, M_g, \quad (19)$$

with the MMSE matrix given in (18) simplified to

$$\mathbb{E} \left\{ \left(\mathbf{h}_k^{i_0} - \widehat{\mathbf{h}}_k^{i_0} \right) \left(\mathbf{h}_k^{i_0} - \widehat{\mathbf{h}}_k^{i_0} \right)^H \right\} = \left(1 - \sigma_0^2 \right) \mathbf{I}_N, \quad i = 1, 2, \dots, M_g. \quad (20)$$

C. Estimation of Other Columns in Each Group

For the j -th column ($j = 2, 3, \dots, M_e$) in the i -th group, the channel vector $\mathbf{h}_k^{(M_e(i-1)+j)}$ can also be estimated by using the CSI table Φ_k^i and the antenna position information $z_k^{(M_e(i-1)+j)}$. For clarity, we denote $i_0 = M_e(i-1) + 1$ and $j_0 = M_e(i-1) + j$ in this subsection. As observed from Fig. 3, $z_k^{j_0}$ is located between $z_{k_0}^{i_0}$ and $z_{k_0+1}^{i_0}$ along the moving path, namely $|z_k^{i_0} - z_{k_0}^{i_0}| \geq |z_k^{j_0} - z_{k_0}^{i_0}| \geq |z_k^{j_0} - z_{k_0+1}^{i_0}|$. The value of k_0 can be obtained by comparing $z_k^{j_0}$ with $\{z_l^{i_0}, l = 1, 2, \dots, k\}$ that is contained in Φ_k^i . In particular, on the condition that the transmitter is in uniform motion with speed v_0 and the interval between two adjacent antennas is $\frac{\lambda_0}{2}$, $|z_m^{i_0} - z_n^{i_0}| = \frac{|m-n|v_0T_0}{B_0}$. Then, by using $|z_k^{j_0} - z_{k_0}^{i_0}| = \frac{(j-1)\lambda_0}{2}$, the above condition becomes

$$\frac{(k - k_0)v_0T_0}{B_0} \geq \frac{(j-1)\lambda_0}{2} \geq \frac{(k - k_0 - 1)v_0T_0}{B_0} \quad (21)$$

$$\Rightarrow k_0 = \left\lfloor k - \frac{(j-1)\lambda_0 B_0}{2v_0T_0} \right\rfloor. \quad (22)$$

It can be seen that the particular value of k_0 depends on the value of ξ_0 in the expression of $T_0 = \frac{\lambda_0 B_0}{2\xi_0 v_0}$. For instance, $k - k_0 \approx (j-1)\xi_0$, if the effect of the floor operator in (21) is ignored.

As shown in Fig. 3, the next task is to estimate $\mathbf{h}_k^{j_0}$ based on $\{\widehat{\mathbf{g}}_{k-L_0+1}^i, \dots, \widehat{\mathbf{g}}_{k_0}^i, \widehat{\mathbf{g}}_{k_0+1}^i, \dots, \widehat{\mathbf{g}}_{k_0+L_0}^i\}$ aided by the position information. Similarly as before, $\widehat{\mathbf{g}}_{k-L_0+1}^i, \dots, \widehat{\mathbf{g}}_{k_0}^i, \widehat{\mathbf{g}}_{k_0+1}^i, \dots, \widehat{\mathbf{g}}_{k_0+L_0}^i$ and $\mathbf{h}_k^{j_0}$ are jointly Gaussian distributed, with the covariance matrix

$$\begin{aligned} \mathbf{R}_{\widehat{\mathbf{g}}_{k_0+L_0}^i, \dots, \widehat{\mathbf{g}}_{k_0+1}^i, \mathbf{h}_k^{j_0}, \widehat{\mathbf{g}}_{k_0}^i, \dots, \widehat{\mathbf{g}}_{k-L_0+1}^i} &= \begin{pmatrix} \mathbf{R}_{\widehat{\mathbf{g}}_{k+L_0}^i} & \cdots & \mathbf{R}_{\widehat{\mathbf{g}}_{k+L_0}^i \mathbf{h}_k^{j_0}} & \cdots & \mathbf{R}_{\widehat{\mathbf{g}}_{k+L_0}^i \widehat{\mathbf{g}}_{k-L_0+1}^i} \\ \vdots & \ddots & & & \\ \mathbf{R}_{\mathbf{h}_k^{j_0} \widehat{\mathbf{g}}_{k+L_0}^i} & \cdots & \mathbf{R}_{\mathbf{h}_k^{j_0}} & \cdots & \mathbf{R}_{\mathbf{h}_k^{j_0} \widehat{\mathbf{g}}_{k-L_0+1}^i} \\ \vdots & & & \ddots & \\ \mathbf{R}_{\widehat{\mathbf{g}}_{k-L_0+1}^i \widehat{\mathbf{g}}_{k+L_0}^i} & \cdots & \mathbf{R}_{\widehat{\mathbf{g}}_{k-L_0+1}^i \mathbf{h}_k^{j_0}} & \cdots & \mathbf{R}_{\widehat{\mathbf{g}}_{k-L_0+1}^i} \end{pmatrix} \\ &= \begin{pmatrix} \mathbf{R}_1 & \mathbf{r}_1^H & \mathbf{R}_2 \\ \mathbf{r}_1 & 1 & \mathbf{r}_2 \\ \mathbf{R}_2^H & \mathbf{r}_2^H & \mathbf{R}_1 \end{pmatrix} \otimes \mathbf{I}_N, \end{aligned} \quad (23)$$

with

$$\mathbf{R}_1 = \begin{pmatrix} \eta_{1,1} \sigma_0^2 & \eta_{1,2} \sigma_0^4 & \cdots & \eta_{1,L_0} \sigma_0^4 \\ \eta_{2,1} \sigma_0^4 & \eta_{2,2} \sigma_0^2 & \cdots & \eta_{2,L_0} \sigma_0^4 \\ \vdots & & \ddots & \\ \eta_{L_0,1} \sigma_0^4 & \eta_{L_0,2} \sigma_0^4 & \cdots & \eta_{L_0,L_0} \sigma_0^2 \end{pmatrix}, \quad (24)$$

$$\mathbf{R}_2 = \begin{pmatrix} \eta_{1,L_0+1} \sigma_0^4 & \eta_{1,L_0+2} \sigma_0^4 & \cdots & \eta_{1,2L_0} \sigma_0^4 \\ \eta_{2,L_0+1} \sigma_0^4 & \eta_{2,L_0+2} \sigma_0^4 & \cdots & \eta_{2,2L_0} \sigma_0^4 \\ \vdots & & \ddots & \\ \eta_{L_0,L_0+1} \sigma_0^4 & \eta_{L_0,L_0+2} \sigma_0^4 & \cdots & \eta_{L_0,2L_0} \sigma_0^4 \end{pmatrix}, \quad (25)$$

$$\mathbf{r}_1 = [\eta'_{L_0} \sigma_0^2, \eta'_{L_0-1} \sigma_0^2, \dots, \eta'_2 \sigma_0^2, \eta'_1 \sigma_0^2], \quad (26)$$

$$\mathbf{r}_2 = [\eta''_1 \sigma_0^2, \eta''_2 \sigma_0^2, \dots, \eta''_{L_0-1} \sigma_0^2, \eta''_{L_0} \sigma_0^2], \quad (27)$$

where

$$\eta'_l = J_0 \left(2\pi \frac{|z_k^{j_0} - z_{k_0+l}^{i_0}|}{\lambda_0} \right), \quad (28)$$

$$\eta''_l = J_0 \left(2\pi \frac{|z_k^{j_0} - z_{k_0-l+1}^{i_0}|}{\lambda_0} \right). \quad (29)$$

The MMSE estimate of $\mathbf{h}_k^{j_0}$ is given by

$$\begin{aligned}\widehat{\mathbf{h}}_k^{j_0} &= \mathbb{E} \left\{ \mathbf{h}_k^{j_0} \left| \widehat{\mathbf{g}}_{k-L_0+1}^i, \dots, \widehat{\mathbf{g}}_{k_0}^i, \widehat{\mathbf{g}}_{k_0+1}^i, \dots, \widehat{\mathbf{g}}_{k_0+L_0}^i \right. \right\} \\ &= \begin{pmatrix} \mathbf{r}_1 & \mathbf{r}_2 \end{pmatrix} \begin{pmatrix} \mathbf{R}_1 & \mathbf{R}_2 \\ \mathbf{R}_2^T & \mathbf{R}_1 \end{pmatrix}^{-1} \otimes \mathbf{I}_N \begin{pmatrix} \widehat{\mathbf{g}}_{k_0+L_0}^i \\ \vdots \\ \widehat{\mathbf{g}}_{k_0-L_0+1}^i \end{pmatrix}.\end{aligned}\quad (30)$$

Again the estimate is a linear combination of the $2L_0$ samples in Φ_k^i and the interpolation coefficients can be precomputed offline. The corresponding MMSE matrix is given by

$$\mathbb{E} \left\{ (\mathbf{h}_k^{j_0} - \widehat{\mathbf{h}}_k^{j_0})(\mathbf{h}_k^{j_0} - \widehat{\mathbf{h}}_k^{j_0})^H \right\} = \mathbf{I}_N - \begin{pmatrix} \mathbf{r}_1 & \mathbf{r}_2 \end{pmatrix} \begin{pmatrix} \mathbf{R}_1 & \mathbf{R}_2 \\ \mathbf{R}_2^H & \mathbf{R}_1 \end{pmatrix}^{-1} \begin{pmatrix} \mathbf{r}_1 \\ \mathbf{r}_2 \end{pmatrix} \otimes \mathbf{I}_N. \quad (31)$$

Specifically, for the case of $L_0 = 1$, $\widehat{\mathbf{h}}_k^{j_0}$ can be simplified as

$$\begin{aligned}\widehat{\mathbf{h}}_k^{j_0} &= \mathbb{E} \left\{ \mathbf{h}_k^{j_0} \left| \widehat{\mathbf{g}}_{k_0+1}^i, \widehat{\mathbf{g}}_{k_0}^i \right. \right\} \\ &= \begin{pmatrix} \eta_1' \sigma_0^2 & \eta_1'' \sigma_0^2 \end{pmatrix} \begin{pmatrix} \sigma_0^2 & \eta_1 \sigma_0^4 \\ \eta_1 \sigma_0^4 & \sigma_0^2 \end{pmatrix}^{-1} \begin{pmatrix} \widehat{\mathbf{g}}_{k_0+1}^i \\ \widehat{\mathbf{g}}_{k_0}^i \end{pmatrix} \\ &= \frac{\eta_1'' - \eta_1 \eta_1' \sigma_0^2}{1 - \eta_1^2 \sigma_0^4} \widehat{\mathbf{g}}_{k_0+1}^i + \frac{\eta_1' - \eta_1 \eta_1'' \sigma_0^2}{1 - \eta_1^2 \sigma_0^4} \widehat{\mathbf{g}}_{k_0}^i,\end{aligned}\quad (32)$$

where $\eta_1 = J_0 \left(2\pi \frac{|z_{k_0+1}^{i_0} - z_{k_0}^{i_0}|}{\lambda_0} \right)$, $\eta_1' = J_0 \left(2\pi \frac{|z_k^{j_0} - z_{k_0+1}^{i_0}|}{\lambda_0} \right)$ and $\eta_1'' = J_0 \left(2\pi \frac{|z_k^{j_0} - z_{k_0}^{i_0}|}{\lambda_0} \right)$ based on (28).

Finally, the MMSE matrix in (31) can be simplified as

$$\mathbb{E} \left\{ \widetilde{\mathbf{h}}_k^{j_0} (\widetilde{\mathbf{h}}_k^{j_0})^H \right\} = \left(1 - \sigma_0^2 \cdot \Gamma(\eta_1, \eta_1', \eta_1'') \right) \mathbf{I}_N, \quad (33)$$

where

$$\Gamma(\eta_1, \eta_1', \eta_1'') = \frac{\eta_1'^2 + \eta_1''^2 - 2\eta_1 \eta_1' \eta_1'' \sigma_0^2}{1 - \eta_1^2 \sigma_0^4}. \quad (34)$$

Remark 2: It is worth noting again that there is no spatial correlation between antenna elements due to sufficiently separation. Namely, $\mathbf{h}_k^1, \mathbf{h}_k^2, \dots, \mathbf{h}_k^M$ are independent of each other, so the results of [12] based on the correlation structure among $\mathbf{h}_k^1, \mathbf{h}_k^2, \dots, \mathbf{h}_k^M$ can not be applied. However, based on *Assumption 1*, we can establish the relationship between $\mathbf{h}_k^{j_0}$ and $\widehat{\mathbf{g}}_{k_0+1}^i, \widehat{\mathbf{g}}_{k_0}^i$ (the past estimates of the first transmit antenna in the same group) by utilizing the joint spatio-temporal correlation in (3) with the help of position information of the transmit antenna array. Thus, we can get the estimator in (32) and reduce the training overhead.

D. Summary and Comments

In summary, for the k -th signal block, the channel estimation process consists of the following steps:

- Step 1: The first transmit antenna of each group transmits pilot symbols. The receiver computes the initial estimate $\widehat{\mathbf{G}}_k$ based on (9) and (10) using the received signals and updates the M_g CSI tables $\Phi_k^i = [\Phi_{k-1}^i, (\widehat{\mathbf{g}}_k^i, z_k^{(M_e(i-1)+1)})]$, $i = 1, 2, \dots, M_g$.
- Step 2: The estimate of the first column $\mathbf{h}_k^{(M_e(i-1)+1)}$ in the i -th sub-matrix \mathbf{Q}_k^i is refined by using (17), $i = 1, 2, \dots, M_g$.
- Step 3: The estimate of the j -th column $\mathbf{h}_k^{(M_e(i-1)+j)}$ in the i -th sub-matrix \mathbf{Q}_k^i , $j = 2, 3, \dots, M_e$, is computed by using (30). This yields the estimate of the entire channel matrix $\widehat{\mathbf{H}}_k = [\widehat{\mathbf{h}}_k^1, \widehat{\mathbf{h}}_k^2, \dots, \widehat{\mathbf{h}}_k^M]$.

Remark 3: (Maximum value for M_e) Since the channel state over the moving path is estimated by the pilot symbols from the first transmit antenna in a group and the estimation results are finally reused by the last antenna in the same group, the time interval between which is $\Delta T = \frac{(M_e-1)\lambda_0}{2v_0}$. In order to guarantee that the channel state at a fixed point does not change during this period, ΔT should be less than the coherence time of the transmission environment t_0 , i.e., $\frac{(M_e-1)\lambda_0}{2v_0} < t_0$. Thus, the maximum allowable value for M_e can be expressed as

$$M_e = \left\lfloor \frac{2v_0 t_0}{\lambda_0} + 1 \right\rfloor. \quad (35)$$

Remark 4: It is seen that the value of M_e is bounded, especially when the speed v_0 is low. It means that the size of the antenna array is limited if we only employ one group, which will lead to a low throughput. So, in order to support a larger size of antenna array, multiple groups should be employed. The optimal value of M_g will be considered in Section IV.D.

IV. PERFORMANCE ANALYSIS AND THROUGHPUT OPTIMIZATION

A. Effective SNR Analysis

Denote $\widetilde{\mathbf{H}}_k = \mathbf{H}_k - \widehat{\mathbf{H}}_k$ as the channel estimation error. The data phase in the k -th block is

$$\mathbf{Y}_{d,k} = \sqrt{\frac{P_d}{M}} \widehat{\mathbf{H}}_k \mathbf{S}_{d,k} + \sqrt{\frac{P_d}{M}} \widetilde{\mathbf{H}}_k \mathbf{S}_{d,k} + \mathbf{V}_{d,k}, \quad (36)$$

where P_d denotes the transmit power in the data phase, $\mathbf{V}_{d,k}$ is an additive white Gaussian noise term with i.i.d. $\mathcal{CN}(0, 1)$ elements, while $\mathbf{S}_{d,k} \in \mathbb{C}^{M \times T_d}$ and $\mathbf{Y}_{d,k} \in \mathbb{C}^{N \times T_d}$ are the transmitted signal and received signal, respectively.

Since $\widehat{\mathbf{H}}_k$ is an MMSE estimate, the error $\widetilde{\mathbf{H}}_k$ is uncorrelated with $\widehat{\mathbf{H}}_k$ due to the orthogonality principle [30]. Let $\mathbf{E}_{d,k} = \sqrt{\frac{P_d}{M}} \widetilde{\mathbf{H}}_k \mathbf{S}_{d,k} + \mathbf{V}_{d,k}$ be an equivalent additive noise term that combines the effects of channel noise and channel estimation error. It follows that $\mathbf{E}_{d,k}$ is also zero mean and uncorrelated with $\widehat{\mathbf{H}}_k \mathbf{S}_{d,k}$. It is known that for uncorrelated additive noise, the worst distribution in terms of capacity is Gaussian [6, 28, 29]. Thus, on the condition that the transmitted signal satisfies $\mathbb{E}\{\mathbf{S}_{d,k} \mathbf{S}_{d,k}^H\} = T_d \mathbf{I}_M$, a lower bound on the capacity during the data phase can be expressed as

$$C_{\text{worst}} = \mathbb{E} \left\{ \log_2 \det \left(\mathbf{I}_N + \frac{P_d}{M} \mathbf{R}_E^{-1} \widehat{\mathbf{H}}_k \widehat{\mathbf{H}}_k^H \right) \right\}, \quad (37)$$

where $\mathbf{R}_E = \frac{1}{T_d} \mathbb{E}\{\mathbf{E}_{d,k} \mathbf{E}_{d,k}^H\} = \frac{P_d}{M} \mathbb{E}\{\widetilde{\mathbf{H}}_k \widetilde{\mathbf{H}}_k^H\} + \mathbf{I}_N$.

In what follows, for tractability of analysis, we focus on the special case of $L_0 = 1$ and the performance of the case with $L_0 > 1$ will be examined via simulations in the next section. Specifically, when $L_0 = 1$, the estimation errors are given by (20) and (33). We have the following result.

Proposition 1: $\Gamma(\eta_1, \eta_1', \eta_1'') > 1$ ($\Gamma(\cdot)$ defined in (34)), if the signal to noise ratio (SNR) during the training phase is less than a certain threshold value, namely $\frac{P_\tau T_\tau}{M_g} < \frac{\Omega}{1-\Omega}$, where

$$\Omega = \min_{\{z_k^{j_0}, j_0=1,2,\dots,M\}} \frac{2\eta_1 \eta_1' \eta_1'' - \sqrt{4\eta_1^2 \eta_1'^2 \eta_1''^2 - 4\eta_1^2 (\eta_1'^2 + \eta_1''^2 - 1)}}{2\eta_1^2}. \quad (38)$$

Proof: See Appendix A. ■

In particular, for the typical system parameter with $\xi_0 = 20$, i.e., $T_0 = \lfloor \frac{\lambda_0 B_0}{40v_0} \rfloor$, it can be obtained that $\Omega = 0.999997609$ and the SNR threshold value $\frac{\Omega}{1-\Omega} = 56.2\text{dB}$. Hence, if the SNR value is below 56.2dB, a very mild condition that always holds in practice, we can obtain $\Gamma(\eta_1, \eta'_1, \eta''_1) > 1$. Then, the MMSE error of the first column in each group given by (20) is larger than that of other columns given by (33).

Remark 5: As shown in Fig. 3, $2L_0$ samples are utilized to estimate $\mathbf{h}_k^{(M_e(i-1)+j)}$ based on (32) while only L_0 samples are utilized to estimate $\mathbf{h}_k^{(M_e(i-1)+1)}$ based on (19) due to the causality constraint. Hence, unless the SNR during training phase is extremely large, the estimation error of the first column is typically larger than that of others in the same group.

Thus, in practice, the estimation error for the first column in each group is the largest compared with that of other columns. We can then obtain a further lower bound on the capacity by assuming that the covariance of the estimation error of any column is $(1 - \sigma_0^2)\mathbf{I}_N$. That is, we can use the following system model to lower bound the capacity of the original system in (36):

$$\mathbf{Y}_{d,k} = \sqrt{\frac{P_d}{M}} \widehat{\mathbf{H}}'_k \mathbf{S}_{d,k} + \sqrt{\frac{P_d}{M}} \widetilde{\mathbf{H}}'_k \mathbf{S}_{d,k} + \mathbf{V}_{d,k}, \quad (39)$$

where $\widehat{\mathbf{H}}'_k$ contains i.i.d. $\mathcal{CN}(0, \sigma_0^2)$ elements while $\widetilde{\mathbf{H}}'_k$ contains i.i.d. $\mathcal{CN}(0, 1 - \sigma_0^2)$ elements, and they are uncorrelated with each other.

For the model in (39), we have $\mathbb{E}\{\widetilde{\mathbf{H}}'_k (\widetilde{\mathbf{H}}'_k)^H\} = M(1 - \sigma_0^2)\mathbf{I}_N$ and $\mathbf{R}_{E'} = \frac{1}{T_d} \mathbb{E}\{\mathbf{E}'_{d,k} (\mathbf{E}'_{d,k})^H\} = \frac{P_d}{M} \mathbb{E}\{\widehat{\mathbf{H}}'_k (\widehat{\mathbf{H}}'_k)^H\} + \mathbf{I}_N = [P_d(1 - \sigma_0^2) + 1]\mathbf{I}_N$. Then, using (37), the lower bound on the capacity of the system in (36) during data phase can be expressed as

$$C_L = \mathbb{E} \left\{ \log_2 \det \left(\mathbf{I}_N + \frac{P_d \sigma_0^2}{1 + P_d(1 - \sigma_0^2)} \cdot \frac{\overline{\mathbf{H}}_k \overline{\mathbf{H}}_k^H}{M} \right) \right\}, \quad (40)$$

where the normalized channel estimate is $\overline{\mathbf{H}}_k = \frac{\widehat{\mathbf{H}}'_k}{\sqrt{\sigma_0^2}}$, consisting of $\mathcal{CN}(0, 1)$ elements.

B. End-to-End Throughput Optimization and System Parameter selections

Taking the training stage into account, we can maximize the system throughput by optimally allocating the channel resources between the training and data phases. That is

$$R_L = \max_{P_d, T_d} \mathbb{E} \left\{ \frac{T_0 - T_\tau}{T_0} \cdot \log_2 \det \left(\mathbf{I}_N + \frac{P_d \sigma_0^2}{1 + P_d(1 - \sigma_0^2)} \cdot \frac{\overline{\mathbf{H}}_k \overline{\mathbf{H}}_k^H}{M} \right) \right\}, \quad (41)$$

where the pre-log factor $\frac{T_0 - T_\tau}{T_0}$ accounts for the estimation cost of channel uses, while P_d and T_d satisfy the following constraints of total time slot and total transmission energy per block:

$$T_0 = T_\tau + T_d, \quad P_0 T_0 = P_\tau T_\tau + P_d T_d. \quad (42)$$

Substituting the expression of σ_0^2 into (41), the effective signal-to-noise ratio (SNR) can be expressed as

$$\rho_{\text{eff}} = \frac{P_d \sigma_0^2}{1 + P_d(1 - \sigma_0^2)} = \frac{P_d \frac{P_\tau}{M_g} T_\tau}{1 + P_d + \frac{P_\tau}{M_g} T_\tau}. \quad (43)$$

In order to maximize the right-hand side of (41) with respect to power allocation and the time interval partition, namely $\{P_\tau, P_d\}$ and $\{T_\tau, T_d\}$, we have the following two Lemmas.

Lemma 1: (Optimal Power Ratio) The optimal power ratio is given by $\frac{P_d}{P_0} = \alpha \frac{T_0}{T_d}$, where

$$\alpha = \frac{\sqrt{T_d(M_g + P_0 T_0)}}{\sqrt{M_g(T_d + P_0 T_0)} + \sqrt{T_d(M_g + P_0 T_0)}}. \quad (44)$$

Proof: See Appendix B. ■

Lemma 2: (Optimal Time Interval Partition) The optimal length of the training interval under the optimal power allocation ratio is M_g for all possible P_0 and T_0 .

Proof: See Appendix C. ■

Then, by substituting the results in *Lemma 1* and *Lemma 2* into (41), we obtain the following conclusion.

Proposition 2: In a training-based system with position-aided channel estimation, the lower bound on the throughput under the optimal channel resource allocation can be expressed as

$$R_L = \mathbb{E} \left\{ \frac{T_0 - M_g}{T_0} \cdot \log_2 \det \left(\mathbf{I}_N + \rho_{\text{eff}}^* \frac{\overline{\mathbf{H}}_k \overline{\mathbf{H}}_k^H}{M} \right) \right\}, \quad (45)$$

where

$$\rho_{\text{eff}}^* = \frac{P_0^2 T_0^2}{[\sqrt{M_g(T_0 - M_g + P_0 T_0)} + \sqrt{(T_0 - M_g)(M_g + P_0 T_0)}]^2}, \quad (46)$$

$$T_0 = \left\lfloor \frac{\lambda_0 B_0}{2\xi_0 \nu_0} \right\rfloor.$$

C. Special Case: $M_e = 1$ —Conventional Training Scheme

If we set $M_e = 1$ (and $M_g = M$), the position-aided channel estimator will reduce to the conventional channel estimator. To serve as a baseline, let us analyze the performance of conventional training. Substituting $M_e = 1$ and $M_g = M$ into (45) and (46), we can obtain the corresponding performance of the conventional training scheme, which is consistent with the prior work [6].

Corollary 1: *In a training-based system with conventional training, the lower bound on the throughput under well-designed system parameters can be expressed as*

$$R_L = \mathbb{E} \left\{ \frac{T_0 - M}{T_0} \cdot \log_2 \det \left(\mathbf{I}_N + \rho_{\text{eff}}^* \frac{\overline{\mathbf{H}}_k \overline{\mathbf{H}}_k^H}{M} \right) \right\}, \quad (47)$$

where

$$\rho_{\text{eff}}^* = \frac{P_0^2 T_0^2}{[\sqrt{M(T_0 - M + P_0 T_0)} + \sqrt{(T_0 - M)(M + P_0 T_0)}]^2}. \quad (48)$$

D. Optimal Antenna Size

Lastly, we consider the optimal size of the antenna array for the system with the proposed position-aided estimation scheme. It is assumed that the number of receive antennas is always equal to that of transmit antennas. Since the total number of transmit antennas is $M = M_e \cdot M_g$ and the value of M_e is given by (35), it remains to determine the value of M_g . We consider this problem from the viewpoint of maximizing the multiplexing gain of the system, namely the degrees-of-freedom (DoF) of the system, which is defined as follows [31]

$$\text{DoF} = \lim_{P_0 \rightarrow \infty} \frac{R_L}{\log_2 P_0} \quad (49)$$

Proposition 3: *For a training-based system with position-aided channel estimation, the optimal number of transmit antennas M^* in terms of maximizing DoF is*

$$M^* = \frac{T_0}{2} \cdot M_e, \quad (50)$$

i.e., $M_g^* = \frac{T_0}{2}$ and M_e is given by (35).

Proof: See the Appendix D. ■

Similar to *Proposition 3*, we can get the optimal number of transmit antennas for the conventional training system by setting $M_e = 1$ and $M_g = M$, which is summarized as follows.

Corollary 2: *For the training-based system with conventional training, the optimal number of transmit antennas in terms of maximizing DoF is*

$$M^* = \frac{T_0}{2}. \quad (51)$$

V. SIMULATION RESULTS

A. Comparison Between Two Training Schemes

We first compare the throughput performance of the proposed position-aided channel estimator to that of the conventional one, the explicit expressions of which are given in (45) and (47), respectively. For the fairness of comparison, we assume that the antenna sizes under the two estimation schemes are the same in this subsection.

Specifically, it is assumed that the carrier wavelength $\lambda_0 = 0.15\text{m}$ (i.e., the carrier frequency is 2GHz), the bandwidth $B_0 = 10\text{MHz}$, the coherence time of environment $t_0 = 5\text{ms}$, and the length of each signal block is equal to the twentieth of the coherence time of channel ($\xi_0 = 20$). The average SNR value is 30dB. We consider the case that the number of receive antennas is the same as that of transmit antennas. Fig. 4 plots the throughput of a training-based system under the proposed position-aided channel estimator and the conventional estimator as a function of the velocity v_0 when the number of antennas M is 100 and 200, respectively. In the system with position-aided channel estimation, the value of M_e is given by (35), and the corresponding M_g is equal to $\lceil \frac{M}{M_e} \rceil$; if the value of M is not a multiple of M_e , some extra zero columns can be added to the end of the last group $\mathbf{Q}_k^{M_g}$ to match with the formulation in (45).

It is seen from Fig. 4 that the throughput of the conventional training scheme deteriorates significantly as the relative velocity increases, especially when the antenna size is large. This is because the training phase occupies too many channel uses. In particular, the throughput can even become zero when the velocity is large enough, which highlights the main motivation of this work to propose the concept of position-aided training: to reduce the estimation overhead

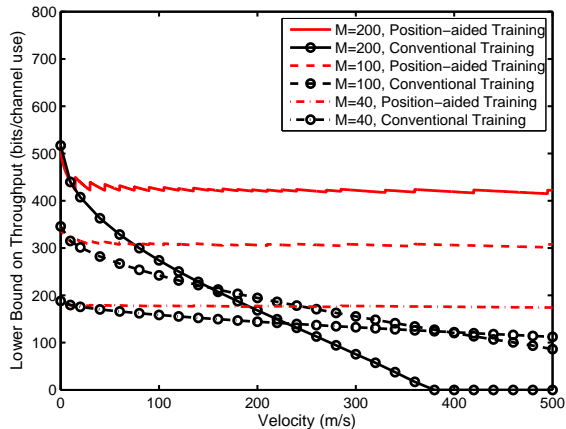


Fig. 4: Throughput comparison between the proposed position-aided channel estimator and the conventional estimator as a function of velocity v_0 when the average SNR is 30dB.

in highly mobile environments. In contrast, the performance of the position-aided estimation scheme deteriorates a little and is nearly independent of the velocity due to the exploitation of the spatio-temporal correlation in a mobile environment. A higher mobility leads to smaller value of T_0 , which reduces the duration of data phase. However, it also makes it possible to group more columns together to share the common training signal based on (35), which can reduce the portion of training phase in a block. As a result, the system with position-aided channel estimation can achieve a robust performance with respect to mobility, even when M is just on the order of tens (such as $M = 40$). Significant improvement can be achieved if we employ position-aided channel estimation for the large-scale MIMO system in the high-speed railway scenarios.

B. Performance Comparison under the Optimal Antenna Array Size

In this subsection, we compare the performance of the two channel estimation schemes under their respective optimal antenna sizes which are given by (50) and (51). Fig. 5 depicts the DoF performance of the training-based system as a function of velocity v_0 with the position-aided training scheme and the conventional training scheme. It can be observed that the DoF

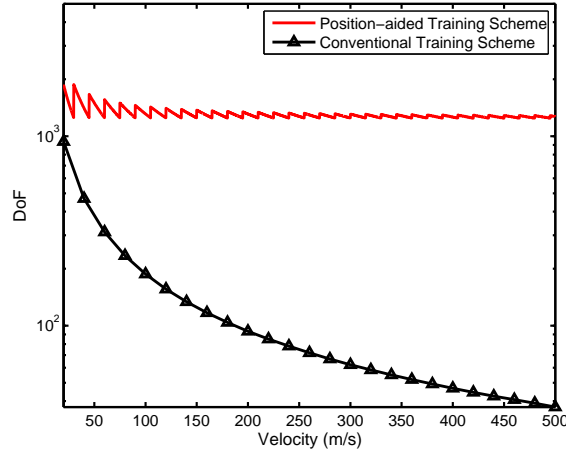


Fig. 5: The DoF of the training-based system with position-aided training and conventional training as a function of velocity v_0 , when the optimal antenna sizes in (50) and (51) are adopted.

with conventional training decreases with the velocity v_0 . The DoF with position-aided channel estimation is significantly higher than that of the conventional one, especially when the speed is high, which is consistent with the results in Fig. 4 for the case of fixed antenna size. It should be noted that the discontinuity phenomenon in the performance curves is caused by the round-off operation in calculating M_e and M_g .

The optimal antenna size M^* in (50) is obtained based on DoF maximization in the high SNR regime. Let us examine the optimality based on numerical simulation when the SNR is not so high. Assuming that the velocity $v_0 = 100\text{m/s}$ and the other parameters are just the same as those in the previous subsection, Fig. 6a depicts the system throughput with position-aided channel estimation as a function of group number M_g under different average SNR values. The ideal optimum group number calculated by (50) is $M_g^* = 375$ as displayed in Fig. 6a. It can be observed that the practical optimal value for M_g is very close to 375 even when the SNR is only 20dB. Likewise, Fig. 6b depicts the throughput under conventional training scheme as a function of antenna size M when $v_0 = 100\text{m/s}$. Similar results can be observed from it.

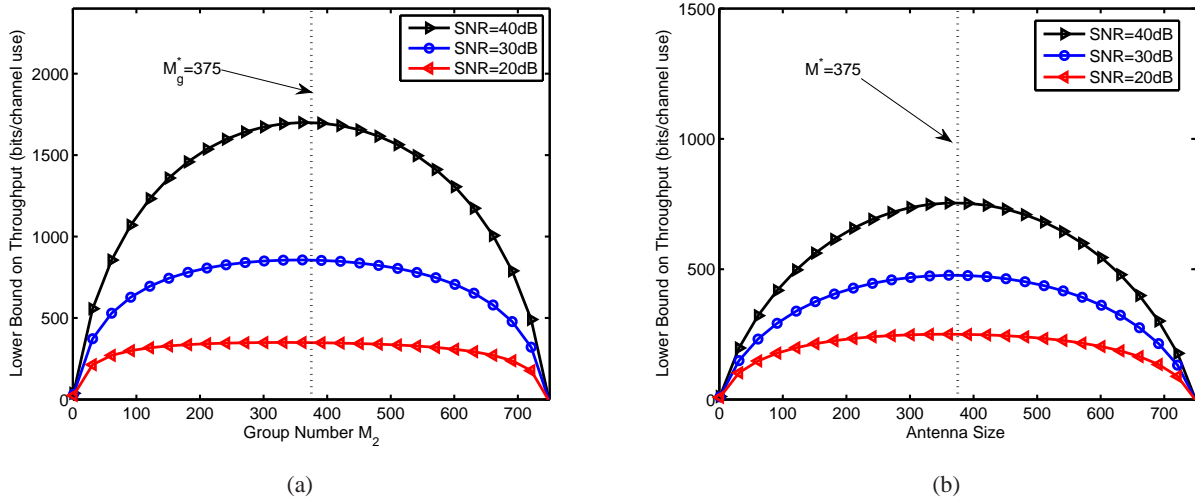


Fig. 6: The system throughput as a function of antenna size M when $v_0 = 100\text{m/s}$: (a) with position-aided channel estimation scheme, (b) with conventional training scheme.

C. Performance with $L_0 > 1$

The analysis in Section IV and the above numerical results concentrate on the case of $L_0 = 1$ in (17) and (30). We now consider the general case with $L_0 > 1$ via simulations. It is assumed that the system parameters are the same as those in Section V.A. The antenna size at the transmitter and receiver are $M = N = 200$. The value of M_e is given by (35) and the corresponding M_g is set as $\lceil \frac{M}{M_e} \rceil$. Fig. 7 plots the system throughput with the position-aided channel estimation as a function of the velocity with $L_0 = 1, 2, 3, 4$ and $SNR = 20\text{dB}$. The training interval in both cases is set as $T_\tau = M_g$. Besides, for a fair comparison, the uniform power distribution is adopted, i.e., $P_\tau = P_d = P_0$. Fig. 8 plots the system throughput under position-aided channel estimation scheme as a function of SNR when the velocity is 100m/s , $M = N = 200$ and $L_0 = 1, 2, 3, 4$. From Figs. 7 and 8, it is seen that there is only a slight gain with $L_0 > 1$ compared with $L_0 = 1$. Thus, we strongly recommend to employ the case with $L_0 = 1$ in a highly mobile large-scale MIMO system, to achieve a considerable improvement with low complexity.

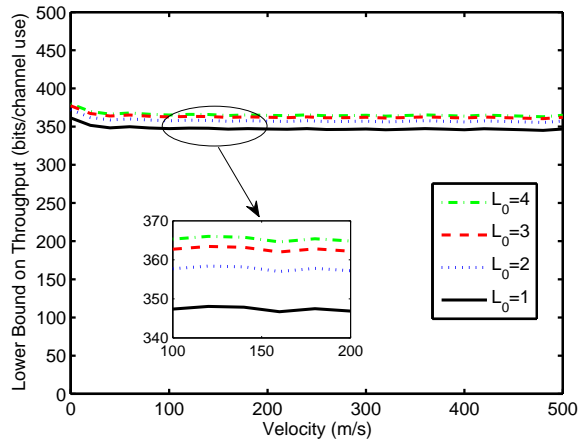


Fig. 7: The system throughput with position-aided channel estimation as a function of velocity for $L_0 = 1, 2, 3, 4$ and $SNR = 20\text{dB}$.

VI. CONCLUSIONS

We have proposed a position-aided channel estimation scheme for training-based large-scale MIMO systems to reduce the pilot overhead in high-speed railway communications. In this concept, only a subset of the transmit antennas need to send pilot symbols during the training phase of each block. The entire channel matrix can be estimated from the initial estimate of the submatrix with the help of position information by exploiting the spatio-temporal correlation structure of the channel. We have also developed a framework of optimizing the training interval, power allocation and antenna size for the proposed position-aided training system. A salient feature of the proposed scheme is that the system throughput remains invariant as the transmitter's moving speed varies, whereas for the system that employs conventional training, the throughput deteriorates rapidly as the speed increases and even becomes zero with very high mobility.

APPENDIX A: PROOF OF PROPOSITION 1

The condition $\Gamma(\eta_1, \eta_1', \eta_1'') > 1$ is equivalent to

$$\frac{\eta_1'^2 + \eta_1''^2 - 2\eta_1\eta_1'\eta_1''\sigma_0^2}{1 - \eta_1^2\sigma_0^4} > 1. \quad (52)$$

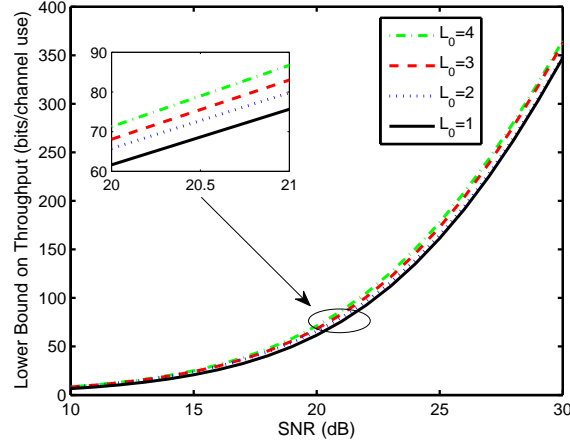


Fig. 8: The system throughput with position-aided channel estimation as a function of SNR for $L_0 = 1, 2, 3, 4$ and $v_0 = 100\text{m/s}$.

Since both η_1 and σ_0^2 belong to $(0, 1)$, we have $1 - \eta_1^2 \sigma_0^4 > 0$. By some manipulations, (52) is equivalent to

$$\eta_1^2 \sigma_0^4 - 2\eta_1 \eta_1' \eta_1'' \sigma_0^2 + (\eta_1'^2 + \eta_1''^2 - 1) > 0 \quad (53)$$

$$\Rightarrow \sigma_0^2 \in \left(0, \frac{2\eta_1 \eta_1' \eta_1'' - \sqrt{4\eta_1^2 \eta_1'^2 \eta_1''^2 - 4\eta_1^2 (\eta_1'^2 + \eta_1''^2 - 1)}}{2\eta_1^2} \right). \quad (54)$$

From (28), it can be seen that η_1' and η_1'' are functions of $z_{k_0}^{i_0}$, $z_k^{j_0}$ and $z_{k_0+1}^{i_0}$, the values of which are different for different columns. In order to guarantee that $\Gamma(\eta_1, \eta_1', \eta_1'') > 1$, we then need $\sigma_0^2 \in (0, \Omega)$, where

$$\Omega = \min_{\{z_k^{j_0}, j_0=1,2,\dots,M\}} \frac{2\eta_1 \eta_1' \eta_1'' - \sqrt{4\eta_1^2 \eta_1'^2 \eta_1''^2 - 4\eta_1^2 (\eta_1'^2 + \eta_1''^2 - 1)}}{2\eta_1^2}. \quad (55)$$

Thus, $\Gamma(\eta_1, \eta_1', \eta_1'') > 1$, if the SNR value during the training phase meets the following constraint on the condition

$$\frac{P_\tau T_\tau}{M_g} < \frac{\Omega}{1 - \Omega}. \quad (56)$$

APPENDIX B: PROOF OF LEMMA 1

As observed from (41)–(43), the power allocation strategy $\{P_\tau, P_d\}$ only affects the throughput via ρ_{eff} . Thus, maximizing ρ_{eff} with respect to (P_τ, P_d) is equivalent to maximizing R_L . We use

a similar formulation as that in [6]. That is, letting α be the fraction of total transmit energy that is dedicated to data phase, we have

$$P_d T_d = \alpha P_0 T_0, \quad P_\tau T_\tau = (1 - \alpha) P_0 T_0, \quad 0 < \alpha < 1. \quad (57)$$

Then, we can rewrite the effective SNR in (43) as

$$\rho_{\text{eff}} = \frac{P_d \frac{P_\tau}{M_g} T_\tau}{1 + P_d + \frac{P_\tau}{M_g} T_\tau} = \frac{\alpha \frac{P_0 T_0}{M_g T_d} (1 - \alpha) P_0 T_0}{1 + \alpha \frac{P_0 T_0}{T_d} + (1 - \alpha) \frac{P_0 T_0}{M_g}} = \frac{P_0^2 T_0^2}{\frac{M_g(T_d + P_0 T_0)}{1 - \alpha} + \frac{T_d(M_g + P_0 T_0)}{\alpha}}. \quad (58)$$

Denote $\mathfrak{L}(\alpha) = \frac{M_g(T_d + P_0 T_0)}{1 - \alpha} + \frac{T_d(M_g + P_0 T_0)}{\alpha}$. As a result, minimizing $\mathfrak{L}(\alpha)$ is equivalent to maximizing ρ_{eff} . We have

$$\frac{\partial \mathfrak{L}}{\partial \alpha} = \frac{M_g(T_d + P_0 T_0)}{(1 - \alpha)^2} - \frac{T_d(M_g + P_0 T_0)}{\alpha^2}, \quad (59)$$

$$\frac{\partial^2 \mathfrak{L}}{\partial \alpha^2} = 2 \cdot \frac{M_g(T_d + P_0 T_0)}{(1 - \alpha)^3} + 2 \cdot \frac{T_d(M_g + P_0 T_0)}{\alpha^3}. \quad (60)$$

Since $\frac{\partial^2 \mathfrak{L}}{\partial \alpha^2} > 0$, $\mathfrak{L}(\alpha)$ is convex and has an unique minimum, which is

$$\mathfrak{L}_{\min} = \left[\sqrt{M_g(T_d + P_0 T_0)} + \sqrt{T_d(M_g + P_0 T_0)} \right]^2. \quad (61)$$

By solving $\frac{\partial \mathfrak{L}}{\partial \alpha} = 0$, we obtain

$$\alpha^* = \frac{\sqrt{T_d(M_g + P_0 T_0)}}{\sqrt{M_g(T_d + P_0 T_0)} + \sqrt{T_d(M_g + P_0 T_0)}}. \quad (62)$$

APPENDIX C: PROOF OF LEMMA 2

Let us consider the monotonicity of the throughput function R_L in (41) with respect to the variable T_d under the optimal power allocation presented in *Lemma 1*. Plugging (44) into (43), the effective SNR with optimal power allocation can be rewritten as

$$\rho_{\text{eff}} = \frac{P_0^2 T_0^2}{\left[\sqrt{M_2(T_d + P_0 T_0)} + \sqrt{T_d(M_2 + P_0 T_0)} \right]^2}. \quad (63)$$

Assuming λ_i is the i -th nonnegative singular value of the matrix $\frac{\overline{H}_k \overline{H}_k^*}{M}$, the throughput function can be expressed as

$$R = \sum_i \mathbb{E} \left\{ \frac{T_d}{T_0} \cdot \ln \left(1 + \rho_{\text{eff}} \lambda_i \right) \right\}, \quad (64)$$

where we use the natural logarithm to instead of \log_2 for convenience, and the expectation operation is over λ_i .

Let $R_i(T_d)$ be $\mathbb{E}\left\{\frac{T_d}{T_0} \cdot \ln(1 + \rho_{\text{eff}}\lambda_i)\right\}$. The first order derivative of $R_i(T_d)$ with respect to T_d is

$$\frac{\partial R_i(T_d)}{\partial T_d} = \mathbb{E}\left\{\frac{1}{T_0} \log_2(1 + \rho_{\text{eff}}\lambda_i) + \frac{T_d}{T_0} \frac{\lambda_i}{1 + \rho_{\text{eff}}\lambda_i} \frac{\partial \rho_{\text{eff}}}{\partial T_d}\right\}, \quad (65)$$

where

$$\begin{aligned} \frac{\partial \rho_{\text{eff}}}{\partial T_d} &= -\frac{P_0^2 T_0^2 \cdot [2\sqrt{M_g(T_d + P_0 T_0)} + 2\sqrt{T_d(M_g + P_0 T_0)}]}{\{[\sqrt{M_g(T_d + P_0 T_0)} + \sqrt{T_d(M_g + P_0 T_0)}]^2\}^2} \cdot \left[\frac{\sqrt{M_g}}{2\sqrt{T_d + P_0 T_0}} + \frac{1}{2} \frac{\sqrt{M_g + P_0 T_0}}{\sqrt{T_d}}\right] \\ &= \frac{1}{T_d} \cdot \frac{P_0^2 T_0^2}{[\sqrt{M_g(T_d + P_0 T_0)} + \sqrt{T_d(M_g + P_0 T_0)}]^2} \\ &\quad \cdot \frac{[\sqrt{M_g(T_d + P_0 T_0)} + \sqrt{T_d(M_g + P_0 T_0)}] \cdot \left[\frac{T_d \sqrt{M_g}}{\sqrt{T_d + P_0 T_0}} + \sqrt{T_d(M_g + P_0 T_0)}\right]}{[\sqrt{M_g(T_d + P_0 T_0)} + \sqrt{T_d(M_g + P_0 T_0)}]^2}. \end{aligned} \quad (66)$$

Because

$$\frac{T_d \sqrt{M_g}}{\sqrt{T_d + P_0 T_0}} < \sqrt{M_g(T_d + P_0 T_0)}, \quad (67)$$

we have

$$\begin{aligned} &[\sqrt{M_g(T_d + P_0 T_0)} + \sqrt{T_d(M_g + P_0 T_0)}] \cdot \left[\frac{T_d \sqrt{M_g}}{\sqrt{T_d + P_0 T_0}} + \sqrt{T_d(M_g + P_0 T_0)}\right] \\ &< [\sqrt{M_g(T_d + P_0 T_0)} + \sqrt{T_d(M_g + P_0 T_0)}]^2. \end{aligned} \quad (68)$$

Substituting (68) into (66), we can get

$$-\frac{T_d \partial \rho_{\text{eff}}}{\partial T_d} < \rho_{\text{eff}}. \quad (69)$$

Besides, the function $\ln(1 + x) - x/(1 + x) \geq 0$ for all $x \geq 0$, since it is zero at $x = 0$ and an increasing function for $x \geq 0$. Thus, combining the results in (65) and (69), we can get

$$\frac{1}{T_0} \left[\ln(1 + \rho_{\text{eff}}\lambda_i) - \frac{\rho_{\text{eff}}\lambda_i}{1 + \rho_{\text{eff}}\lambda_i} \right] \geq 0. \quad (70)$$

Thus,

$$\frac{\partial R_i(T_d)}{\partial T_d} = \mathbb{E}\left\{\frac{1}{T_0} \log_2(1 + \rho_{\text{eff}}\lambda_i) + \frac{T_d}{T_0} \frac{\lambda_i}{1 + \rho_{\text{eff}}\lambda_i} \frac{\partial \rho_{\text{eff}}}{\partial T_d}\right\} \geq 0. \quad (71)$$

In summary, based on (71), $R_i(T_d)$ is a monotonically increasing function with respect to T_d for arbitrary λ_i . Thus, the throughput function R_L in (64) is a monotonically increasing function

with respect to T_d . To get better performance, T_d should be as large as possible. Thus, the optimal training interval is equal to the number of group M_g in the proposed position-aided group training scheme, which is the minimum value that is required for learning the matrix \mathbf{G}_k .

APPENDIX D: PROOF OF PROPOSITION 3

Using (45) and (46), and assuming that $M = N$, we can get

$$\begin{aligned} R_L &= \frac{T_0 - M_g}{T_0} \cdot \mathbb{E} \left\{ \log_2 \det \left(\mathbf{I}_N + \rho_{\text{eff}}^* \frac{\overline{\mathbf{H}}_k \overline{\mathbf{H}}_k^H}{M} \right) \right\} \\ &= \frac{T_0 - M_g}{T_0} \cdot \sum_{i=1}^{M_e \cdot M_g} \mathbb{E} \left\{ \log_2 \left(1 + P_0 \cdot \frac{P_0 T_0^2}{[\sqrt{M_g(T_0 - M_g + P_0 T_0)} + \sqrt{(T_0 - M_g)(M_g + P_0 T_0)}]^2} \cdot \lambda_i^2 \right) \right\}, \end{aligned} \quad (72)$$

where λ_i^2 denotes the i -th singular value of $\frac{\overline{\mathbf{H}}_k \overline{\mathbf{H}}_k^H}{M}$.

Hence, we have

$$\begin{aligned} \lim_{P_0 \rightarrow \infty} R_L &= \frac{T_0 - M_g}{T_0} \cdot M_e \cdot M_g \left[\log_2 P_0 + o(\log_2 P_0) \right] \\ &= \left\{ - \left(M_g - \frac{T_0}{2} \right)^2 + \frac{T_0^2}{4} \right\} \cdot \frac{M_e \cdot [\log_2 P_0 + o(\log_2 P_0)]}{T_0}. \end{aligned} \quad (73)$$

where $o(x)$ is defined as $\lim_{x \rightarrow 0} \frac{o(x)}{x} = 0$.

Then, the degrees-of-freedom metric becomes

$$\text{DoF} = \lim_{P_0 \rightarrow \infty} \frac{R_L}{\log_2 P_0} = \left\{ - \left(M_g - \frac{T_0}{2} \right)^2 + \frac{T_0^2}{4} \right\} \cdot \frac{M_e}{T_0}. \quad (74)$$

which is maximized by $M_g^* = \frac{T_0}{2}$.

REFERENCES

- [1] A. Goldsmith, S. A. Jafar, N. Jindal, et al, "Capacity limits of MIMO channels," *IEEE J. Sel. Areas Commun.*, vol. 21, no. 5, pp. 684–702, Jun. 2003.
- [2] W. Luo, X. Fang, M. Cheng, et al., "Efficient multiple-group multiple-antenna (MGMA) scheme for high-speed railway viaducts," *IEEE Trans. Veh. Technol.*, vol. 62, no. 6, pp. 2558–2569, Feb. 2013.
- [3] J. Wang, H. Zhu, and N. J. Gomes, "Distributed antenna systems for mobile communications in high speed trains," *IEEE J. Sel. Areas Commun.*, vol. 30, no. 4, pp. 1675–683, May. 2012.
- [4] A. Ghazal, C. X. Wang, B. Ai, et al., "A non-stationary wideband MIMO channel model for high-mobility intelligent transportation systems," *IEEE Trans. Intell. Transp. Syst.*, vol. 16, no. 2, pp. 885–897, Apr. 2015.

- [5] M. S. Pan, T. M. Lin, and W. T. Chen, "An enhanced handover scheme for mobile relays in LTE-A high-speed rail networks," *IEEE Trans. Veh. Technol.*, vol. 64, no. 2, pp. 743–756, Feb. 2015.
- [6] B. Hassibi and B. M. Hochwald, "How much training is needed in multiple-antenna wireless links?" *IEEE Trans. Inf. Theory*, vol. 49, no. 4, pp. 951–963, Apr. 2003.
- [7] J. Heath and W. Robert, "What is the role of MIMO in future cellular networks: Massive? coordinated? mmwave?," *Presentation delivered at IEEE Int. Conf. on Commun. (ICC)*, 2013.
- [8] E. Larsson, O. Edfors, F. Tufvesson, et al, "Massive MIMO for next generation wireless systems," *IEEE Commun. Mag.*, vol. 52, no. 2, pp. 186–195, Feb. 2014.
- [9] C. Kominakis, C. Fragouli, A. Sayed, et al., "Multi-input multi-output fading channel tracking and equalization using Kalman estimation," *IEEE Trans. Signal Process.*, vol. 50, no. 5, pp. 1065–1075, Dec. 2010.
- [10] W. Santipach and M. L. Honig, "Optimization of training and feedback overhead for beamforming over block fading channels," *IEEE Trans. Inf. Theory*, vol. 56, no. 12, pp. 6103–6115, Dec. 2010.
- [11] G. Taubock, F. Hlawatsch, D. Eiwen, and H. Rauhut, "Compressive estimation of doubly selective channels in multicarrier systems: Leakage effects and sparsity-enhancing processing," *IEEE J. Sel. Top. Signal Process.*, vol. 4, no. 2, pp. 255–271, Apr. 2010.
- [12] E. Bjornson and B. Ottersten, "A framework for training-based estimation in arbitrarily correlated Rician MIMO channels with Rician disturbance," *IEEE Trans. Signal Process.*, vol. 58, no. 3, pp. 1807–1820, Mar. 2010.
- [13] J. Choi, D. J. Love and P. Bidigare, "Downlink training techniques for FDD massive MIMO systems: Open-loop and closed-loop training with memory," *IEEE J. Sel. Top. Signal Process.*, vol. 8, no. 5, pp. 802–814, Oct. 2014.
- [14] I. Stojmenovic, "Position-based routing in ad hoc networks," *IEEE Commun. Mag.*, vol. 40, no. 7, pp. 128–134, Jul. 2002.
- [15] Z. Wang, L. Liu, M. C. Zhou, et al. "A position-based clustering technique for ad hoc intervehicle communication," *IEEE Trans. Syst. Man Cybern., C, Appl. Rev.*, vol. 38, no. 2, pp. 201–208, Mar. 2008.
- [16] T. Li, P. Y. Fan and K. B. Letaief, "QoS-distinguished achievable rate region for high speed railway wireless communications," *In Proc. IEEE WCNC 2015*, New Orleans, USA, 2015.
- [17] S. Xu, G. Zhu, C. Shen, et al., "Utility-based resource allocation in high-speed railway wireless networks," *Eurasip J. Wireless Commun. Networking*, vol. 2014, no. 68, pp. 1–14, Apr. 2014.
- [18] L. Liu, C. Tao, J. Qiu, et al., "Position-based modeling for wireless channel on high-speed railway under a viaduct at 2.35 GHz," *IEEE J. Sel. Areas Commun.*, vol. 30, no. 4, pp. 834–845, May. 2012.
- [19] A. Ghazal, C. X. Wang, H. Haas, et al., "A non-stationary geometry-based stochastic model for MIMO high-speed train channels," *In Proc. 2012 12th Int. Conf. on ITS Telecom. (ITST)*, 2012, pp. 7–11.
- [20] X. Ren, W. Chen, and M. X. Tao, "Position-based compressed channel estimation and pilot design for high-mobility OFDM systems," *IEEE Trans. Veh. Technol.*, vol. 64, no. 5, pp. 1918–1929, May. 2015.

- [21] M. Sternad, M. Grieger, R. Apelfrojd, et al., "Using predictor antennas for long-range prediction of fast fading for moving relays," *In Proc. IEEE Wireless Communications and Networking Conference Workshops*, Paris, France, Apr. 2012, pp. 253–257.
- [22] N. Jamaly, R. Apelfrojd, A. B. Martinez, et al., "Analysis and measurement of multiple antenna systems for fading channel prediction in moving relays," *In Proc. IEEE 8th European Conference on Antennas and Propagation (EuCAP)*, Jague, Dutch, Apr. 2014, pp. 2015–2019.
- [23] Z. Zhang, C. Jiao, C. Zhong, et al., "Differential Modulation Exploiting the Spatial-Temporal Correlation of Wireless Channels With Moving Antenna Array," *IEEE Trans. Commun.*, vol. 63, no. 12, pp. 4990–5001, Dec. 2015.
- [24] T. Han, and N. Ansari, "RADIATE: radio over fiber as an antenna extender for high-speed train communications," *IEEE Wirel. Commun.*, vol. 22, no. 1, pp. 130–137, Feb. 2015.
- [25] A. Abdi and M. Kaveh, "A space-time correlation model for multielement antenna systems in mobile fading channel," *IEEE J. Sel. Areas Commun.*, vol. 20, no. 3, pp. 550–560, Apr. 2002.
- [26] T. E. Bogale, L. B. Le, X. B. Wang, et al., "Pilot Contamination Mitigation for Wideband Massive MIMO: Number of Cells Vs Multipath," *In Proc. IEEE GLOBECOM2015*, San Diego, USA, Dec. 2015.
- [27] D. Tse, and P. Viswanath, *Fundamentals of wireless communication*, Cambridge university press, 2005.
- [28] M. Medard, "The effect upon channel capacity in wireless communications of perfect and imperfect knowledge of the channel," *IEEE Trans. Inf. Theory*, vol. 46, no. 3, pp. 933–946, May. 2000.
- [29] A. Lapidoth and S. Shamai, "Fading channels: how perfect need perfect side information be?," *IEEE Trans. Inf. Theory*, vol. 48, no. 5, pp. 1118–1134, May. 2002.
- [30] S. M. Kay, *Fundamentals of Statistical Signal Processing: Estimation Theory*, Upper Saddle River, NJ: Prentice-Hall, 1993.
- [31] L. Z. Zheng and D. N. C. Tse, "Diversity and multiplexing: a fundamental tradeoff in multiple-antenna channels," *IEEE Trans. Inf. Theory*, vol. 49, no. 5, pp. 1073–1096, May. 2003.